

Approximate Implicitization Using Monoid Curves and Surfaces

Thomas W. Sederberg¹, Jianmin Zheng^{1,2}, Kris Klimaszewski¹, Tor Dokken³

¹Department of Computer Science, Brigham Young University, Provo, Utah 84602, USA

²Department of Applied Mathematics, Zhejiang University, Hangzhou 310027, P.R. China

³SINTEF Applied Mathematics, P.O. Box 124 Blindern, N-0134 Oslo, Norway

To be submitted to CVGIP: Graphical Models and Image Processing

June 30, 1998

Running head: Approximate Implicitization Using Monoids

Corresponding Author:

Prof. Thomas W. Sederberg
Department of Computer Science
Brigham Young University
Provo, Utah 84602
Phone: (801)-378-6330
Email: tom@cs.byu.edu

Abstract

This paper presents an approach to finding an approximate implicit equation and an approximate inversion map of a planar rational parametric curve or a rational parametric surface. High accuracy of the approximation is achieved with a relatively small number of low-degree curve segments or surface patches. By using monoid curves and surfaces, the method eliminates the undesirable singularities and “phantom” branches, normally associated with implicit representation. The monoids are expressed in exact implicit and parametric equations simultaneously, and upper bounds are derived for the approximate errors of implicitization and inversion equations.

Keywords: Implicitization, inversion map, approximation, monoid.

List of Symbols

1. Mathematical Operators

$\sqrt{\quad}$	\circ	\min	\neq	\leq	$\bar{\mathbf{P}}$	Σ	\bullet
$\ \quad \ $	$!$	\max	\geq	$\binom{n}{i}$	$\bar{\mathbf{p}}$	$\binom{n}{ijk}$	
$[\quad]$	\in	$ \quad $	\equiv	$[\quad]$	$\bar{\mathbf{r}}$	$\binom{n}{ijkl}$	

2. Greek Characters and other symbols

α	β	Λ	δ	λ	γ	τ	ϵ
μ	ω	ν	Ω	σ	\ddot{o}	\acute{e}	

3. Blackface characters

I	P	p	s	x	r	R	b
----------	----------	----------	----------	----------	----------	----------	----------

4. Characters may have superscripts

$(1 - u)$	γ	τ	v	u	$(1 - u_1)$	(Db)
$(1 - v)$	x	x	y	t	$(1 - v_1)$	D
$(1 - t)$	α	β	h	s	$(1 - \tau)$	$(m + 1)$
$[T - 1 - T_0, T_2 - T_0]$			$[T - 1 - T_0, T_2 - T_0, T_3 - T_0]$			

5. Characters may have subscripts

t	T	σ	μ	c	Σ
v	P	ω	u	w	f
ϵ	$\bar{\mathbf{P}}$	s	x	y	$\ \quad \ $
z	Q	b	M	a	ν

6. Symbols may have subscripts and superscripts

B	σ	ω
-----	----------	----------

7. Symbols in superscripts may be Arabic numerals and the following

i	j	nm	k	(m)
n	l	km	τ	$n-1$
I	$\frac{(m+1)(m+2)}{2} - 1$	$\frac{(m+1)(m+2)(m+3)}{6} - 1$		$\lfloor \frac{1}{6} \sqrt{9+12m^3+72m^2+132m} - \frac{1}{2} \rfloor$

8. Symbols in subscripts may be Arabic numerals and the following

I	i	$00n$	ijk	$ijk0$	$i-1,j,k,1$
α	b	$n00$	nm	$i,j-1,1$	$i,j,k-1,1$
μ	j	$0n0$	$ijk1$	$i,j-1,k,1$	$i-1,j,1$
ν	P	$ij0$	ij	$i,j,k,0$	$n-i,i-1,1$
t	Q	$ij1$	$ijkl$	$n-i,i,0$	$n-1-i,i,1$

1 Introduction

Parametric and implicit representations are two main forms for curves and surfaces in CAGD [13]. Each representation has its own advantages. The availability of both often results in simpler computer graphics and geometric modeling algorithms [4, 14, 15, 21].

Classic algebraic geometry reveals that each parametric curve and surface has an implicit representation, while the converse is not true [23]. The process of converting the parametric equation into the implicit form is called implicitization. Many techniques, such as the resultant-based method [20], Gröbner basis method [5], and moving curve and surface methods [22], have been developed to implicitize parametric curves and surfaces.

However, implicitization (especially surface implicitization) has not found widespread use in geometric modeling. This is in part due to the fact that the surface implicitization process is relatively complicated and the degree of the implicit surface equation high. Another difficulty is that a single implicitized parametric curve or surface may have unwanted components or self-intersections. Figure 1a shows a cubic Bézier curve with the control polygon, and Figure 1b shows the implicitized curve with a double point. Figure 2 shows a quartic Bézier curve and its implicit curve, which includes an extraneous curve segment in the neighborhood of the Bézier curve. These undesirable extraneous singularities and branches often lead to computational instability and topological inconsistency in geometric modeling, thus limiting the usefulness of implicitization.

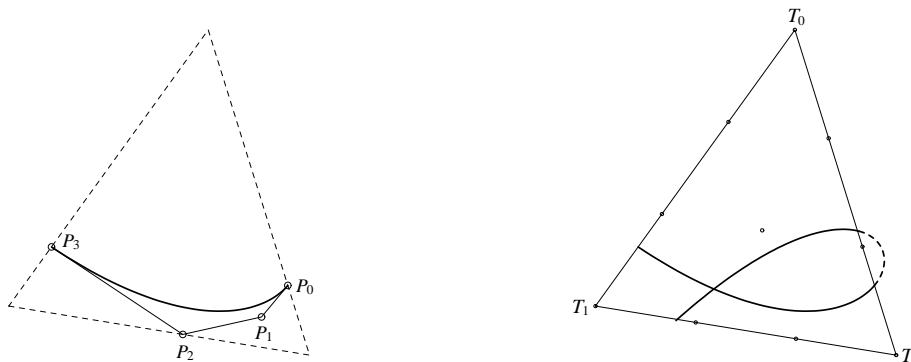


Figure 1: a). Cubic Bézier curve and its control polygon; b). Implicit curve with a double point.

For these reasons, approximate implicitization has been proposed [6, 9, 25]. Montaudouin and Tiller employed a power series method to obtain local explicit approximations — about a regular point — to polynomial

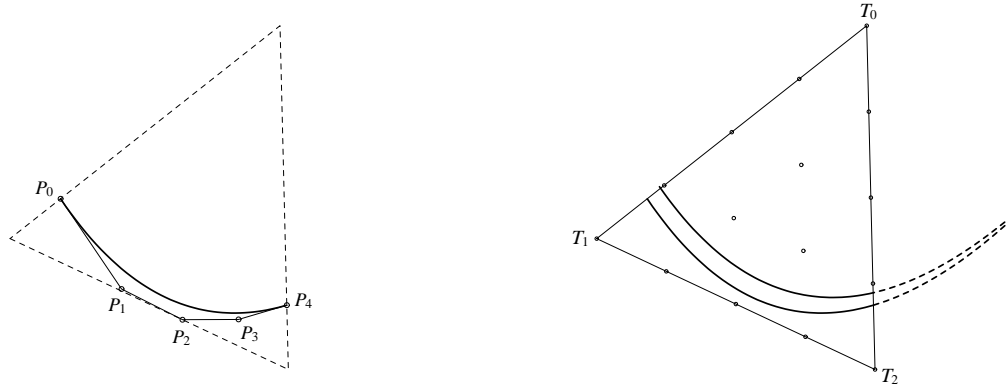


Figure 2: a). Quartic Bézier curve and its control polygon; b). Implicit curve with a “phantom” branch.

parametric curves and surfaces [9]. This approach is asymmetric as one variable is made an explicit function of the other(s). Chuang and Hoffmann extended this method using what they call “implicit approximation” [6]. A low-degree implicit equation is computed to locally approximate a properly—parametrized rational curve or surface. In this way one can obtain the exact implicit form if the approximant is of the same degree as the implicit form. Dokken proposed a new way to approximate the parametric curve and surface “globally” in the sense that the approximation is valid within the whole domain of the curve segment or surface patch. An in-depth investigation of this topic can be found in his dissertation [11]. But, even these approximate implicitization methods can suffer from the problems illustrated in Figures 1 and 2. To circumvent these difficulties, algorithms based on monotonicity and least-squares approximation can be invoked [2, 7, 8, 12] and certain constraints on the coefficients of the implicit representation [1, 3, 18, 19] have been introduced.

This paper most closely extends Dokken’s work to approximate implicitization as well as approximate inversion map, and proposes employing monoid curves and surfaces to compute a low-degree approximant. This allows us to overcome the two problems mentioned earlier. Moreover, monoids have another advantage in that they possess both exact implicit and parametric representations.

The paper is organized as follows. Section 2 reviews some of Dokken’s approximate implicitization results. In section 3, we present the development of the monoid curve scheme, including the dual representation of the monoid curve, approximate implicitization, approximate inversion map and error analysis. Section 4 describes monoid surface case. Examples and some observations are given in section 5.

2 Approximate implicitization method

Dokken developed a general method to approximately implicitize g -manifolds represented by parametric equations [11]. Here, we outline his approach.

Let $\mathbf{p}(\mathbf{s})$ be a parametric — say, Bézier — curve or surface. We would like to find an *approximate* low-degree implicit equation $q(\mathbf{x}) = 0$ for $\mathbf{p}(\mathbf{s})$. In general, the distance between the parametric curve or surface and its implicit approximation depends not only on the value of $q \circ \mathbf{p}(\mathbf{s})$, but also on the gradient of $q(\mathbf{x})$. However, in practice, the value of $|q \circ \mathbf{p}(\mathbf{s})|$ alone can serve as a measure of the goodness of an approximation, provided the coefficients of q are normalized. This reduces the implicitization problem to finding a degree m algebraic hypersurface $q(\mathbf{x}) = 0$ with normalized coefficients such that $|q \circ \mathbf{p}(\mathbf{s})| \leq \epsilon$, where ϵ is a prescribed tolerance.

Let S be an arbitrary simplex containing $\mathbf{p}(\mathbf{s})$, and $q(\mathbf{x}) = \sum_I b_I \frac{m!}{I!} \mathbf{x}^I$ be represented in barycentric coordinates \mathbf{x} over S . Then the composition of $q(\mathbf{x}) = 0$ and $\mathbf{p}(\mathbf{s})$ can be expressed as

$$q \circ \mathbf{p}(\mathbf{s}) = (Db)^T \Lambda(\mathbf{s}), \quad (1)$$

where D is a constant matrix, called *composite matrix*, b is a vector consisting of the coefficients of q , and $\Lambda(\mathbf{s})$ is a vector whose components are basis functions of the composition.

If the components of $\Lambda(\mathbf{s})$ form a unit partition for $\mathbf{s} \in \Omega$, the following properties hold:

Property 1. $\max_{\mathbf{s} \in \Omega} |q \circ \mathbf{p}(\mathbf{s})| \leq \|Db\|_2$

Property 2. $\min_{\|b\|_2=1} \|Db\|_2 = \sigma_1$, where $\sigma_1 \geq 0$ is the smallest singular value of D .

Thus we can obtain $q(\mathbf{x})$ by setting b to the eigenvector of $D^T D$ that corresponds to the eigenvalue σ_1^2 . This will ensure $q(\mathbf{x})$ satisfies $|q \circ \mathbf{p}(\mathbf{s})| \leq \epsilon$ when $\sigma_1 < \epsilon$.

Dokken has proven theoretically that the convergence rates for approximating planar parametric curves, space parametric curves and surfaces by their algebraic counterparts are respectively $O(h^{\frac{(m+1)(m+2)}{2}-1})$, $O(h^{\frac{(m+1)(m+2)(m+3)}{6}-1})$ and $O(h^{\lfloor \frac{1}{6} \sqrt{9+12m^3+72m^2+132m} - \frac{1}{2} \rfloor})$, with h being the diameter of the parameter domain. For example, the approximation for a planar curve has a convergence rate of 5 for $m = 2$, of 9 for $m = 3$ and of 14 for $m = 4$. This remarkably high rate implies that good accuracy is achievable when even a small number of low-degree curves and surfaces are used.

Example 2.1. Let $C(v) = (x(v)/w(v), y(v)/w(v))$, $v \in [0, 1]$ be a degree 8 rational curve:

$$\begin{cases} x(v) &= 52.7v^8 - 237.8v^7 + 445.5v^6 - 447.4v^5 + 273.8v^4 - 117.6v^3 + 28v^2 + 8.8v - 2.2 \\ y(v) &= -29.8v^8 + 96.7v^7 - 122.9v^6 + 68.3v^5 + 4.9v^4 - 38.6v^3 + 36.7v^2 - 11.4v + 0.6 \\ w(v) &= 2.9v^8 - 7.2v^7 + 16.8v^5 - 21v^4 + 11.2v^3 - 2.8v^2 + 1.1 \end{cases}$$

and $S(u, v) = (-0.08u^3v^3 + 0.33u^2v^3 + 0.24u^3v + 0.48u^3 - 0.99u^2v - 0.25v^3 - 1.98u^2 + 0.75v + 1.5, -0.08u^3v^3 - 0.09u^2v^3 + 0.24u^3v + 0.42uv^3 + 0.48u^3 + 0.27u^2v + 0.54u^2 - 1.26uv - 2.52u, 0.075v^3 - 1.57v + 2.4)$ be a bicubic patch. We compute the approximate implicitization using degree 3 algebraic curves and surfaces. We also subdivide the curve and the surface, and process the approximate implicitization for each sub-segment and sub-patch. The absolute values of the compositions and the approximation errors are shown in Table 1.

subdivision level	Curve		Surface	
	$ q \circ C(v) \leq$	Dist \leq	$ q \circ S(u, v) \leq$	Dist \leq
0	3×10^{-4}	1×10^{-2}	1.6×10^{-5}	2.3×10^{-4}
1	8×10^{-6}	7×10^{-5}	7.8×10^{-6}	4.1×10^{-5}
2	6×10^{-8}	5×10^{-7}	1.3×10^{-6}	2.8×10^{-6}

Table 1: Approximation errors by algebraic curves and surfaces.

3 Monoid curves

Since curves are conceptually and notationally simpler and easier to visualize than surfaces, we begin our discussion with the former.

A degree n algebraic curve is defined by an implicit equation which is normally written in the standard power basis:

$$f(x, y) = \sum_{i+j \leq n} f_{ij} x^i y^j = 0. \quad (2)$$

However, it is convenient to express such an equation in Bernstein-Bézier form relative to an arbitrary triangle, called the curve's *reference triangle*, in the plane $z = 0$ using barycentric coordinates (s, t, u) :

$$f(s, t, u) = \sum_{i+j+k=n} c_{ijk} \binom{n}{ijk} s^i t^j u^k = 0, \quad s + t + u \equiv 1. \quad (3)$$

In this formulation [18], the curve can be viewed as the intersection of the plane $z = 0$ with the triangular Bézier surface patch

$$\begin{pmatrix} x \\ y \\ z \end{pmatrix} = \sum_{i+j+k=n} \mathbf{P}_{ijk} \binom{n}{ijk} s^i t^j u^k, \quad 0 \leq s, t, u \leq 1, \quad s + t + u \equiv 1. \quad (4)$$

The projection of control points \mathbf{P}_{ijk} onto the plane $z = 0$ forms a triangular lattice with the reference triangle's vertices T_0 , T_1 and T_2 corresponding to \mathbf{P}_{00n} , \mathbf{P}_{n00} and \mathbf{P}_{0n0} , respectively. That is,

$$\mathbf{P}_{ijk} = \begin{pmatrix} x_{ijk} \\ y_{ijk} \\ z_{ijk} \end{pmatrix} = \begin{pmatrix} (ix_{n00} + jx_{0n0} + kx_{00n})/n \\ (iy_{n00} + jy_{0n0} + ky_{00n})/n \\ c_{ijk} \end{pmatrix}. \quad (5)$$

Note that the reference triangle bounds the intersection of the triangular surface patch with the plane $z = 0$. Using this formulation, it is possible to represent the algebraic curve segments of interest. However, as demonstrated in Figures 1 and 2, the implicitized parametric curves often have self-intersections and undesirable “phantom” components. Since monoid curves and surfaces can easily avoid these problems, our strategy is to use the monoid representation in lieu of general algebraic curves and surfaces.

3.1 Dual representation for monoid curves

An algebraic curve of degree n with a multiple point O of order $n - 1$ was called by Cayley a *monoid* [24]. If O is at the original point, the monoid curve equation consists of terms of degree n and $n - 1$ only. The genus of such a curve is zero, therefore the curve is rational. Also, as any line through O meets the curve in just one other point, there is a one-to-one correspondence between the points on the curve and the pencil of lines with the axis located at O .

In the Bernstein-Bézier formulation, a monoid curve has a simple representation if we choose one vertex of the reference triangle to be the multiple point. Let a degree n monoid curve be defined by (3) in the Bernstein-Bézier form over reference triangle $T_0T_1T_2$. If we assume T_0 to be the multiple point of the monoid curve, then $c_{ijk} = 0$ when $k > 1$ (see Figure 3). Thus the curve equation can be rewritten as

$$f(s, t, u) = f_b(s, t) + uf_i(s, t) = \sum_{i+j=n} c_{ij0} \binom{n}{i} s^i t^j + un \sum_{i+j=n-1} c_{ij1} \binom{n-1}{i} s^i t^j. \quad (6)$$

This is the implicit representation of a monoid curve.

We now derive the parametric representation. Let $P(s, t, u)$ be a point on the monoid curve (see Figure 4). Line T_0P will intersect T_1T_2 at point I , whose coordinates are $(s/(1 - u), t/(1 - u), 0)$. By introducing a new parameter $\tau = t/(1 - u)$, the barycentric coordinates of P can be expressed in terms of τ and u :

$$s = (1 - \tau)(1 - u), \quad t = \tau(1 - u), \quad u = u. \quad (7)$$

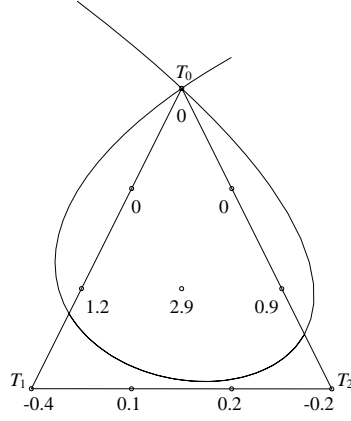


Figure 3: Cubic monoid curve with its double point T_0 .

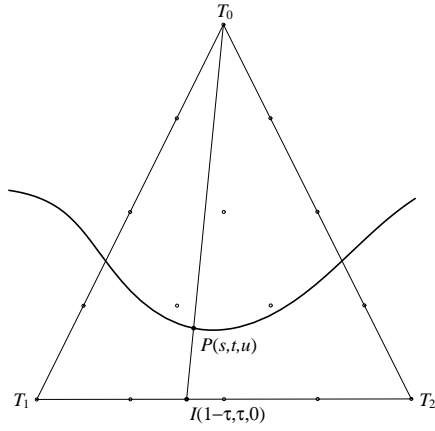


Figure 4: Parameter of a monoid curve.

Furthermore, since $P(s, t, u)$ lies on the curve, it satisfies the implicit equation

$$f_b(s, t) + uf_i(s, t) = (1 - u)^n f_b(1 - \tau, \tau) + u(1 - u)^{n-1} f_i(1 - \tau, \tau) = 0. \quad (8)$$

In consequence,

$$\begin{cases} s = \frac{-(1 - \tau)f_i(1 - \tau, \tau)}{f_b(1 - \tau, \tau) - f_i(1 - \tau, \tau)}; \\ t = \frac{-\tau f_i(1 - \tau, \tau)}{f_b(1 - \tau, \tau) - f_i(1 - \tau, \tau)}; \\ u = \frac{f_b(1 - \tau, \tau)}{f_b(1 - \tau, \tau) - f_i(1 - \tau, \tau)}. \end{cases} \quad (9)$$

This represents a rational parametric curve of degree n . The equation can be further rewritten in the Bézier

form:

$$\begin{pmatrix} s \\ t \\ u \end{pmatrix} = \frac{\sum_{i=0}^n w_i Q_i B_i^n(\tau)}{\sum_{i=0}^n w_i B_i^n(\tau)} \quad (10)$$

with

$$\begin{aligned} &\text{the weights } w_i = c_{n-i,i,0} - i c_{n-i,i-1,1} - (n-i) c_{n-1-i,i,1} \\ &\text{and the control points } Q_i = \begin{pmatrix} -(n-i) c_{n-1-i,i,1} \\ -i c_{n-i,i-1,1} \\ c_{n-i,i,0} \end{pmatrix} / w_i. \end{aligned}$$

If the weights are all non-negative or all non-positive and $w_0 w_n \neq 0$, we say that the coefficients $c_{i,j,k}$ satisfy the “same-sign” condition. Under this condition, the monoid curve has many useful properties, one of which is convex hull property.

Finally, it follows from the above derivation that the inversion map of the monoid curve is a linear fractional transformation

$$\tau = t/(1-u). \quad (11)$$

3.2 Approximate implicitization and inversion map

Given a planar degree n rational Bézier curve

$$\mathbf{p}(v) = \frac{\sum_{i=0}^n \omega_i \mathbf{P}_i B_i^n(v)}{\sum_{i=0}^n \omega_i B_i^n(v)}, \quad v \in [0, 1], \quad (12)$$

where \mathbf{P}_i are the control points, ω_i the weights and $B_i^n(t) = \binom{n}{i} (1-t)^{n-i} t^i$, we want to find a monoid curve $q(\bullet) = 0$ to approximate the parametric curve. The process of approximate implicitization involves the following steps.

1. Determine the reference triangle for the monoid curve.

To define an algebraic curve, an arbitrary triangle can be used as the reference triangle. Dokken showed that the numerical stability of the approximation process benefits from choosing a bounding triangle as the reference triangle. However, for a monoid curve one vertex of the reference triangle must be the multiple point if we express the curve as in (6). When a monoid curve is used to approximate a parametric curve segment, the location of the multiple point has a significant impact on the accuracy of the approximation. As an example, Figure 5 demonstrates the relationship between the maximum approximation error and the location of the multiple point for a cubic Bézier curve.

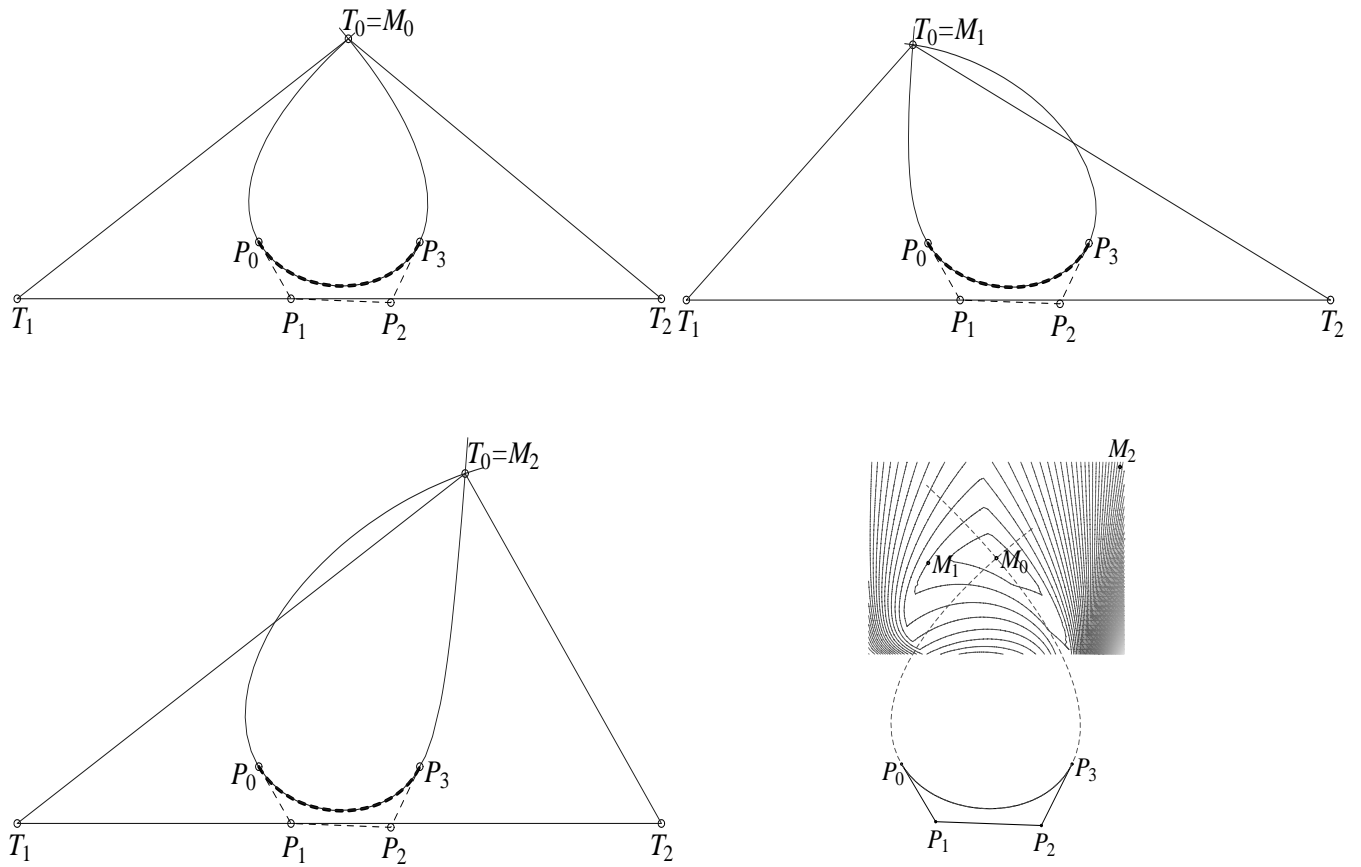


Figure 5: An example of the relationship between the approximation error and the location of the multiple point for a cubic Bézier curve. The errors for the top-left, top-right and bottom-left approximations are 0.0, 0.02, 0.06. The bottom-right figure shows error iso-contours: if T_0 is placed at any point on a contour line, the approximation error is unchanged.

While sampling discretely for the optimal multiple point might give good results, such a search would be computationally expensive. An efficient method of finding the optimal reference triangle (i.e., one that gives the smallest approximation error) is yet to be devised. In the interim, we determine the reference triangle, as shown in Figure 6. First, an oriented bounding box $ABCD$ is computed using a method proposed in [16, 26]. Then we find the “concave” side of the curve segment within that bounding box. (This can be done, somewhat roughly, by classifying the endpoints of the curve segment, P_0 and P_1 , with respect to that axis of symmetry of the bounding box, a_1 , that is parallel to the AB direction.) Next, the

multiple point T_0 is chosen such that it lies on the “concave” side of the curve and on the other axis of symmetry a_2 . Finally, the other vertices of the reference triangle, T_1 and T_2 , are found as the intersections between the bounding box’s base DC and the lines joining the corners A and B with T_0 .

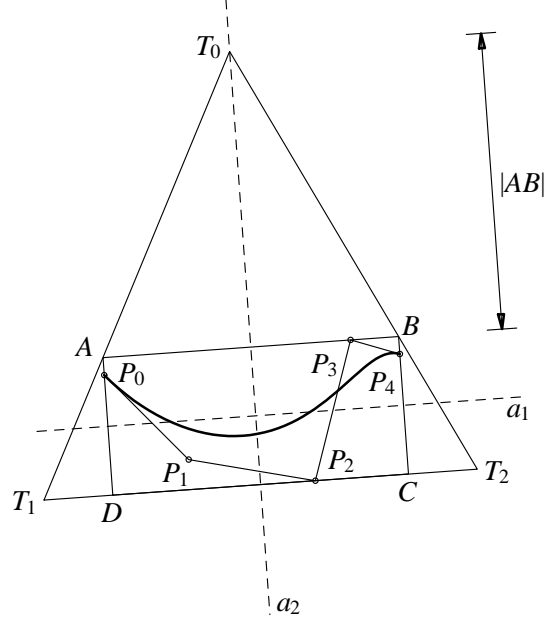


Figure 6: Reference triangle determination.

2. Convert the parametric curve $\mathbf{p}(v)$ into barycentric form.

Let $T_0T_1T_2$ be the reference triangle with T_0 as its multiple point. Then arbitrary point P can be converted into barycentric form

$$P = \begin{pmatrix} x \\ y \end{pmatrix} = sT_1 + tT_2 + uT_0 = T_0 + [T_1 - T_0, T_2 - T_0] \begin{pmatrix} s \\ t \end{pmatrix}, \quad (13)$$

or

$$\begin{cases} \begin{pmatrix} s \\ t \end{pmatrix} &= [T_1 - T_0, T_2 - T_0]^{-1}(P - T_0); \\ u &= 1 - s - t. \end{cases} \quad (14)$$

For a rational Bézier curve, the conversion can be completed simply by applying transformation (14) to each control point \mathbf{P}_i . The converted curve is now put in the form

$$\bar{\mathbf{p}}(v) = \begin{pmatrix} s \\ t \\ u \end{pmatrix} = \frac{\sum_{i=0}^n \omega_i \bar{\mathbf{P}}_i B_i^n(v)}{\sum_{i=0}^n \omega_i B_i^n(v)}, \quad v \in [0, 1]. \quad (15)$$

3. Combine the implicit equation with the parametric equation.

A monoid curve of degree m is defined over reference triangle $T_0T_1T_2$ by

$$q(s, t, u) = \sum_{i+j=m} c_{ij0} \binom{m}{i} s^i t^j + um \sum_{i+j=m-1} c_{ij1} \binom{m-1}{i} s^i t^j. \quad (16)$$

Let \mathbf{b} be a vector consisting of the coefficients of q :

$$\mathbf{b} = [c_{m00}, c_{m-1,1,0}, \dots, c_{0m0}, c_{m-1,0,1}, c_{m-2,1,1}, \dots, c_{0,m-1,1}]^\tau. \quad (17)$$

Substituting the parametric equation $\bar{\mathbf{p}}(v)$ into q leads to

$$q \circ \bar{\mathbf{p}}(v) = (D\mathbf{b})^\tau \Lambda(v), \quad (18)$$

in which $\Lambda(v) = [\omega_0^{(m)} B_0^{nm}(v), \omega_1^{(m)} B_1^{nm}(v), \dots, \omega_{nm}^{(m)} B_{nm}^{nm}(v)]^\tau / \sum_{i=0}^{nm} \omega_i^{(m)} B_i^{nm}(v)$, and D is the composite matrix of order $(mn+1) \times (2m+1)$.

The entries of D can be evaluated by applying the functional composition algorithms [10]. Since $\Lambda(v)$ consists of rational Bernstein polynomials of degree nm , $|q \circ \bar{\mathbf{p}}(v)| \leq \|D\mathbf{b}\|_2$.

4. Perform least-squares approximation.

Usually, the equations $D\mathbf{b} = 0$ are over-constrained. Therefore we seek a least-squares non-zero solution.

Let σ_1^2 be the smallest eigenvalue of $D^\tau D$, and \mathbf{b} a normalized eigenvector of $D^\tau D$ corresponding to σ_1^2 .

Then vector \mathbf{b} is a solution, and the points on the parametric curve are subject to $|q \circ \bar{\mathbf{p}}(v)| \leq \sigma_1$.

In many applications, the inversion formula for a parametric curve is needed. The inversion map of a degree n parametric curve is generally a rational polynomial of degree $n-2$. Having found the reference triangle, we are now in a position to compute an approximate inversion map. To accomplish that, we apply a process similar to our approximate implicitization scheme. Assume that the approximate inversion map is a rational polynomial of degree m ($\leq n-2$):

$$v = \frac{h(s, t, u)}{d(s, t, u)}. \quad (19)$$

To determine the coefficients of the unknown polynomials h and d , we construct a new function

$$H(s, t, u, v) = h(s, t, u) - vd(s, t, u). \quad (20)$$

A least-squares solution for h and d is arrived at by replacing q with H in the steps of our approximate implicitization method.

3.3 Error estimation

3.3.1 Estimation of the distance from a point to a monoid curve

Given a point $P_1(s_1, t_1, u_1)$, we find point P_0 , other than T_0 , at which the monoid curve intersects the line going through T_0 and P_1 (see Figure 7). In order to estimate the smallest distance between P_1 and the curve, we consider the distance from P_1 to P_0 . It is obvious that the former is bounded by the latter.

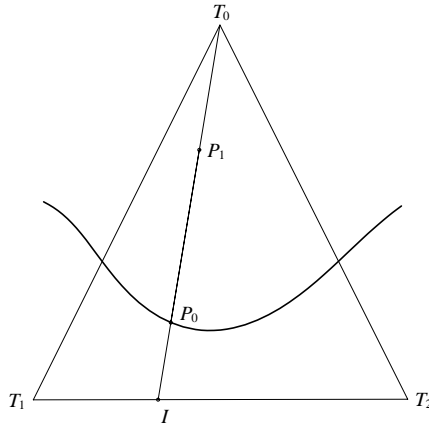


Figure 7: Distance between P_1 and P_0 .

Assume that the barycentric coordinates of P_0 are (s_0, t_0, u_0) and that line T_0P_1 intersects line T_1T_2 at $I(1 - \tau, \tau, 0)$. Hence

$$\begin{aligned} \tau &= t_1/(1 - u_1); \\ s_0 &= (1 - u_0)(1 - \tau), \quad t_0 = (1 - u_0)\tau, \quad u_0 = u_0; \\ s_1 &= (1 - u_1)(1 - \tau), \quad t_1 = (1 - u_1)\tau, \quad u_1 = u_1. \end{aligned} \tag{21}$$

Note that point P_0 is on the monoid curve. From the parametric representation (10),

$$u_0 = f_b(1 - \tau, \tau)/(f_b(1 - \tau, \tau) - f_i(1 - \tau, \tau)). \tag{22}$$

The distance between P_1 and P_0 is :

$$\begin{aligned} \|P_1P_0\| &= \|(s_1 - s_0)T_0T_1 + (t_1 - t_0)T_0T_2\| \\ &= |u_1 - u_0| \|(1 - \tau)T_0T_1 + \tau T_0T_2\| \\ &= |u_1 - \frac{f_b(1-\tau, \tau)}{f_b(1-\tau, \tau) - f_i(1-\tau, \tau)}| \|(1 - \tau)T_0T_1 + \tau T_0T_2\|. \end{aligned} \tag{23}$$

3.3.2 Error bound for approximate implicitization

Assume that $f(P_1) = \epsilon_1$, that is,

$$f(P_1) = (1 - u_1)^{n-1}[(1 - u_1)f_b(1 - \tau, \tau) + u_1f_i(1 - \tau, \tau)] = \epsilon_1. \quad (24)$$

Solving (22) and (24), we have

$$f_b(1 - \tau, \tau) = u_0\epsilon_1 / [(u_0 - u_1)(1 - u_1)^{n-1}], \quad (25)$$

which means

$$u_0 - u_1 = \frac{\epsilon_1}{(1 - u_1)^{n-1}(f_b(1 - \tau, \tau) - f_i(1 - \tau, \tau))}. \quad (26)$$

Using degree elevation, we rearrange $f_b(1 - \tau, \tau) - f_i(1 - \tau, \tau)$:

$$\begin{aligned} f_b(1 - \tau, \tau) &= f_i(1 - \tau, \tau) \\ &= \sum_{i+j=n} c_{ij0} \binom{n}{i} (1 - \tau)^i \tau^j - n \sum_{i+j=n-1} c_{ij1} \binom{n-1}{i} (1 - \tau)^i \tau^j \\ &= \sum_{i+j=n} (c_{ij0} - i c_{i-1,j,1} - j c_{i,j-1,1}) \binom{n}{i} (1 - \tau)^i \tau^j. \end{aligned} \quad (27)$$

When c_{ijk} satisfy the ‘‘same-sign’’ condition mentioned in Section 3.1, $|f_b(1 - \tau, \tau) - f_i(1 - \tau, \tau)| \geq \min_{i+j=n} |c_{ij0} - i c_{i-1,j,1} - j c_{i,j-1,1}|$.

We now turn to estimating the distance between the parametric curve $\mathbf{p}(v)$ and the approximate monoid curve. For the third component of $\mathbf{p}(v)$ in barycentric form (15),

$$1 - u(v) = 1 - \frac{\sum_{i=0}^n \omega_i u_i B_i^n(v)}{\sum_{i=0}^n \omega_i B_i^n(v)} = \frac{\sum_{i=0}^n \omega_i (1 - u_i) B_i^n(v)}{\sum_{i=0}^n \omega_i B_i^n(v)}. \quad (28)$$

Since $\mathbf{p}(v)$ is located within the reference triangle, $1 - u_i > 0$ for all i 's. When all ω_i 's are nonnegative, $|1 - u(v)| \geq \min_i \{1 - u_i\}$.

Consequently, if the above assumptions about coefficients c_{ijk} and weights ω_i hold, an error bound in the approximate implicitization method from Section 3.2 is given by

$$D(\mathbf{p}(v), \text{monoid curve}) \leq \frac{\sigma_1 \max\{\|T_0 T_1\|, \|T_0 T_2\|\}}{\min_i \{1 - u_i\} \min_{i+j=n} |c_{ij0} - i c_{i-1,j,1} - j c_{i,j-1,1}|}. \quad (29)$$

3.3.3 Error bound for approximate inversion map

Once an approximate inversion map

$$v_a = \frac{h(s, t, u)}{d(s, t, u)} \quad (30)$$

is found, substituting the parametric curve equation (15) into it yields

$$h(s(v), t(v), u(v)) - vd(s(v), t(v), u(v)) = \epsilon(v), \quad (31)$$

where $|\epsilon(v)| \leq \sigma_1$, and σ_1 is the smallest singular value of the composite matrix for the composition of H with the parametric curve. Thus the exact parameter is

$$v_t = \frac{h(s, t, u) - \epsilon(v)}{d(s, t, u)}. \quad (32)$$

Hence we find an upper bound on the difference between the exact and approximate parameters:

$$|v_t - v_a| = \left| \frac{\epsilon(v)}{d(s, t, u)} \right| \leq \frac{|\sigma_1|}{\min |d(s, t, u)|}. \quad (33)$$

The value of $\min |d(s, t, u)|$ can generally be estimated using the coefficients of d .

4 Monoid surfaces

Algebraic surfaces suffer from the same problems that algebraic curves do. To remedy these difficulties, we extend the monoid curve scheme to surfaces. Our development parallels that for curves.

4.1 Dual representation for monoid surfaces

A degree n monoid surface has a multiple point O of order $n - 1$, and therefore is rational. For instance, the Steiner surface is a quartic monoid [21]. Just as in the curve case, a *reference tetrahedron* can be specified whose four vertices are denoted by T_0, T_1, T_2 and T_3 . The surface is expressed in Bernstein-Bézier form:

$$f(s, t, u, v) = \sum_{i+j+k+l=n} c_{ijkl} \binom{n}{ijkl} s^i t^j u^k v^l = 0, \quad s + t + u + v \equiv 1, \quad (34)$$

where s, t, u and v are barycentric coordinates with respect to the tetrahedron, and coefficients c_{ijkl} are associated with the so-called control points $P_{ijkl} = \frac{i}{n}T_1 + \frac{j}{n}T_2 + \frac{k}{n}T_3 + \frac{l}{n}T_0$ (see Figure 8).

When T_0 is the multiple point, $c_{ijkl} = 0$ for $l > 1$, and the implicit equation of the monoid surface becomes

$$\begin{aligned} f(s, t, u, v) &= f_b(s, t, u) + v f_i(s, t, u) \\ &= \sum_{i+j+k=n} c_{ijk0} \binom{n}{ijk} s^i t^j u^k + vn \sum_{i+j+k=n-1} c_{ijk1} \binom{n-1}{ijk} s^i t^j u^k. \end{aligned} \quad (35)$$

In order to represent the monoid surface in parametric form, consider an arbitrary point $P(s, t, u, v)$ on the surface. Let I be the intersection point of line T_0P with the plane determined by T_1, T_2 and T_3 . It is easy to

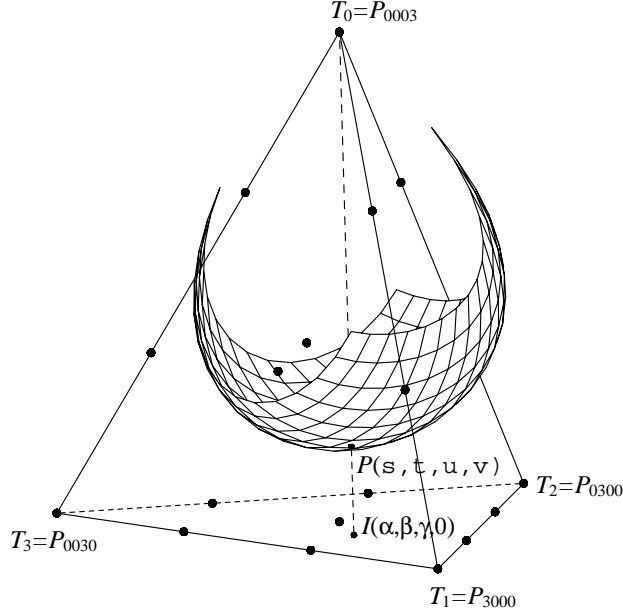


Figure 8: Cubic monoid surface.

show that the barycentric coordinates of I are $(s/(1-v), t/(1-v), u/(1-v), 0)$. Set

$$\alpha = s/(1-v), \quad \beta = t/(1-v), \quad \gamma = u/(1-v) \quad (36)$$

and use α , β and γ as the parameters of the monoid surface

$$s = \alpha(1-v), \quad t = \beta(1-v), \quad u = \gamma(1-v), \quad \alpha + \beta + \gamma \equiv 1. \quad (37)$$

Substituting (37) into (35) yields

$$f_b(s, t, u) + v f_i(s, t, u) = (1-v)^n f_b(\alpha, \beta, \gamma) + v(1-v)^{n-1} f_i(\alpha, \beta, \gamma) = 0. \quad (38)$$

By solving this equation, we obtain the parametric representation for the monoid surface

$$\left\{ \begin{array}{l} s = \frac{-\alpha f_i(\alpha, \beta, \gamma)}{f_b(\alpha, \beta, \gamma) - f_i(\alpha, \beta, \gamma)}, \\ t = \frac{-\beta f_i(\alpha, \beta, \gamma)}{f_b(\alpha, \beta, \gamma) - f_i(\alpha, \beta, \gamma)}, \\ u = \frac{-\gamma f_i(\alpha, \beta, \gamma)}{f_b(\alpha, \beta, \gamma) - f_i(\alpha, \beta, \gamma)}, \\ v = \frac{f_b(\alpha, \beta, \gamma)}{f_b(\alpha, \beta, \gamma) - f_i(\alpha, \beta, \gamma)}. \end{array} \right. \quad (39)$$

Written in triangular Bernstein-Bézier form, it looks like this:

$$\begin{pmatrix} s \\ t \\ u \\ v \end{pmatrix} = \frac{\sum_{i+j+k=n} w_{ijk} Q_{ijk} \binom{n}{ijk} \alpha^i \beta^j \gamma^k}{\sum_{i+j+k=n} w_{ijk} \binom{n}{ijk} \alpha^i \beta^j \gamma^k} \quad (40)$$

with

$$\begin{aligned} &\text{the weights } w_{ijk} = c_{ijk0} - i c_{i-1,j,k,1} - j c_{i,j-1,k,1} - k c_{i,j,k-1,1} \\ &\text{and the control points } Q_{ijk} = \begin{pmatrix} -i c_{i-1,j,k,1} \\ -j c_{i,j-1,k,1} \\ -k c_{i,j,k-1,1} \\ c_{i,j,k,0} \end{pmatrix} / w_{ijk}. \end{aligned}$$

Similarly, the coefficients c_{ijkl} satisfy the “same-sign” condition if the weights w_{ijk} are all non-negative or all non-positive, and the weights at the three corners are nonzero.

4.2 Approximate implicitization and inversion map

We now consider approximate implicitization for a rational Bézier surface of degree $n \times k$ with control points \mathbf{P}_{ij} and weights ω_{ij} :

$$\mathbf{p}(\mu, \nu) = \frac{\sum_{i=0}^n \sum_{j=0}^k \omega_{ij} \mathbf{P}_{ij} B_i^n(\mu) B_j^k(\nu)}{\sum_{i=0}^n \sum_{j=0}^k \omega_{ij} B_i^n(\mu) B_j^k(\nu)}, \quad \mu, \nu \in [0, 1]. \quad (41)$$

In general, the implicit degree of $\mathbf{p}(\mu, \nu)$ is $2mk$. An approximate monoid surface $q(\bullet) = 0$ for this implicit equation can be found using the following procedure.

1. Determine the reference tetrahedron for the monoid surface.

A method for finding the optimum tetrahedron that ensures maximum numerical stability and the best accuracy remains to be discovered. As of now, we are able to propose only an intuitive way of constructing the reference tetrahedron, a direct extension of the approach we used to determine the reference triangle for a curve. Namely, for a given rational parametric Bézier patch, we compute an oriented bounding box and find the “concave” side of the patch. The multiple point is chosen on that side. The other three vertices are determined on the base plane of the bounding box such that the tetrahedron contains the box. Since the construction is similar to that for curves, we omit further details.

2. Convert the parametric surface $\mathbf{p}(\mu, \nu)$ into barycentric form.

If $T_0T_1T_2T_3$ is the reference tetrahedron, then an arbitrary point P can be converted into barycentric form

$$P = \begin{pmatrix} x \\ y \\ z \end{pmatrix} = sT_1 + tT_2 + uT_3 + vT_0 = T_0 + [T_1 - T_0, T_2 - T_0, T_3 - T_0] \begin{pmatrix} s \\ t \\ u \end{pmatrix}, \quad (42)$$

or

$$\begin{cases} \begin{pmatrix} s \\ t \\ u \\ v \end{pmatrix} = [T_1 - T_0, T_2 - T_0, T_3 - T_0]^{-1}(P - T_0); \\ v = 1 - s - t - u. \end{cases} \quad (43)$$

Applied to each control points of $\mathbf{p}(\mu, \nu)$, this transformation produces the surface equation in barycentric form:

$$\bar{\mathbf{p}}(\mu, \nu) = \begin{pmatrix} s \\ t \\ u \\ v \end{pmatrix} = \frac{\sum_{i=0}^n \sum_{j=0}^k \omega_{ij} \bar{\mathbf{P}}_{ij} B_i^n(\mu) B_j^k(\nu)}{\sum_{i=0}^n \sum_{j=0}^k \omega_{ij} B_i^n(\mu) B_j^k(\nu)}. \quad (44)$$

3. Combine the implicit equation with the parametric equation.

A degree m monoid surface defined over reference tetrahedron $T_0T_1T_2T_3$ with multiple point T_0 is expressed by

$$q(s, t, u, v) = \sum_{i+j+k=m} c_{ijk0} \binom{m}{ijk} s^i t^j u^k + vm \sum_{i+j+k=m-1} c_{ijk1} \binom{m-1}{ijk} s^i t^j u^k. \quad (45)$$

Let \mathbf{b} be a vector of the unknown coefficients c_{ijkl} , and $\Lambda(\mu, \nu)$ a vector consisting of the rational polynomial basis $\omega_{ij}^{(m)} B_i^{nm}(\mu) B_j^{km}(\nu) / \sum_{i=0}^{nm} \sum_{j=0}^{km} \omega_{ij}^{(m)} B_i^{nm}(\mu) B_j^{km}(\nu)$. The composition of q and $\bar{\mathbf{p}}(\mu, \nu)$ can now be arranged into

$$q \circ \bar{\mathbf{p}}(\mu, \nu) = (D\mathbf{b})^T \Lambda(\mu, \nu). \quad (46)$$

Matrix D is of order $(mn+1)(km+1) \times (m+1)^2$. We compute its entries using the functional composition algorithm [10]. Note that $q(\bullet)$ satisfies the inequality $|q \circ \bar{\mathbf{p}}(\mu, \nu)| \leq \|D\mathbf{b}\|_2$.

4. Perform least-squares approximation.

To determine the unknown coefficient vector \mathbf{b} , we look for a least-squares non-zero solution to the equations $D\mathbf{b} = 0$. This can be done by computing an eigenvector corresponding to the smallest eigenvalue of $D^T D$. Normalization of this eigenvector yields the solution we seek.

The procedure for approximate implicitization is also valid for finding an approximate inversion equation for $\mathbf{p}(\mu, \nu)$. Assuming that the inversion formulae can be approximated by rational polynomials of degree m

$$\begin{aligned}\mu &= \frac{h(s, t, u, v)}{d(s, t, u, v)}, \\ \nu &= \frac{a(s, t, u, v)}{b(s, t, u, v)},\end{aligned}\tag{47}$$

we construct two functions

$$H(s, t, u, v, \mu, \nu) = h(s, t, u, v) - \mu d(s, t, u, v), \quad G(s, t, u, v, \mu, \nu) = a(s, t, u, v) - \nu b(s, t, u, v),\tag{48}$$

whose total degrees in s, t, u and v are m . Adopting an approach similar to the approximate implicitization method, in which H and G replace q , we arrive at the least-squares solutions for polynomials h, d, a and b .

4.3 Error estimation

4.3.1 Estimation of the distance from a point to a monoid surface

Let us begin by estimating the distance from a given point $P_1(s_1, t_1, u_1, v_1)$ to a monoid surface defined by (35) over the reference tetrahedron $T_0T_1T_2T_3$. The distance is within the length of P_1P_0 . Point $P_0(s_0, t_0, u_0, v_0), v_0 \neq 1$, is the intersection of the surface and line T_0P_1 (see Figure 9).

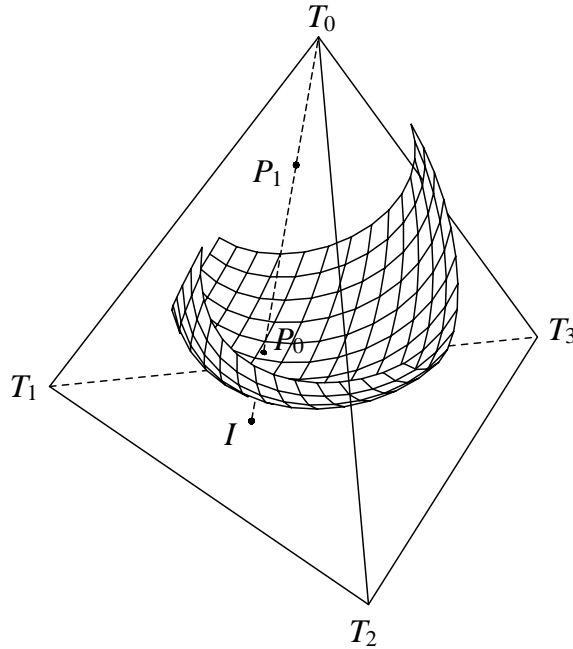


Figure 9: Distance between P_1 and P_0 .

By the monoid's parametric representation (40), we have

$$\begin{aligned}
\alpha &= s_1/(1-v_1), & \beta &= t_1/(1-v_1), & \gamma &= 1-\alpha-\beta; \\
s_0 &= (1-v_0)\alpha, & t_0 &= (1-v_0)\beta, & u_0 &= (1-v_0)\gamma; \\
s_1 &= (1-v_1)\alpha, & t_1 &= (1-v_1)\beta, & u_1 &= (1-v_1)\gamma; \\
v_0 &= f_b(\alpha, \beta, \gamma)/(f_b(\alpha, \beta, \gamma) - f_i(\alpha, \beta, \gamma)).
\end{aligned} \tag{49}$$

From (42) and (49),

$$\begin{aligned}
\|P_1 P_0\| &= \|(s_1 - s_0)T_0 T_1 + (t_1 - t_0)T_0 T_2 + (u_1 - u_0)T_0 T_3\| \\
&= |u_1 - u_0| \|\alpha T_0 T_1 + \beta T_0 T_2 + \gamma T_0 T_3\| \\
&= |u_1 - \frac{f_b(\alpha, \beta, \gamma)}{f_b(\alpha, \beta, \gamma) - f_i(\alpha, \beta, \gamma)}| \|\alpha T_0 T_1 + \beta T_0 T_2 + \gamma T_0 T_3\|.
\end{aligned} \tag{50}$$

4.3.2 Error bound for approximate implicitization

To find how well a monoid surface approximates a given rational parametric surface, let us estimate $|u_1 - u_0|$ first. Assume that $f(P_1) = \epsilon_1$, i.e.,

$$f(P_1) = (1-v_1)^{n-1}[(1-v_1)f_b(\alpha, \beta, \gamma) + v_1 f_i(\alpha, \beta, \gamma)] = \epsilon_1, \tag{51}$$

whence

$$u_0 - u_1 = \frac{\epsilon_1}{(1-v_1)^{n-1}(f_b(\alpha, \beta, \gamma) - f_i(\alpha, \beta, \gamma))}. \tag{52}$$

After using degree elevation,

$$\begin{aligned}
f_b(\alpha, \beta, \gamma) &- f_i(\alpha, \beta, \gamma) \\
&= \sum_{i+j+k=n} c_{ijk0} \binom{n}{ijk} \alpha^i \beta^j \gamma^k - n \sum_{i+j+k=n-1} c_{ijk1} \binom{n-1}{ijk} \alpha^i \beta^j \gamma^k \\
&= \sum_{i+j+k=n} (c_{ijk0} - i c_{i-1,j,k,1} - j c_{i,j-1,k,1} - k c_{i,j,k-1,1}) \binom{n}{ijk} \alpha^i \beta^j \gamma^k.
\end{aligned} \tag{53}$$

When $c_{ijk0} - i c_{i-1,j,k,1} - j c_{i,j-1,k,1} - k c_{i,j,k-1,1}$ all have the same sign, $|f_b(\alpha, \beta, \gamma) - f_i(\alpha, \beta, \gamma)| \geq \min_{i+j+k=n} |c_{ijk0} - i c_{i-1,j,k,1} - j c_{i,j-1,k,1} - k c_{i,j,k-1,1}|$.

Assume that the parametric surface $\mathbf{p}(\mu, \nu)$ is given in the barycentric form (44),

$$1 - v(\mu, \nu) = 1 - \frac{\sum_{i=0}^n \sum_{j=0}^k \omega_{ij} v_{ij} B_i^n(\mu) B_j^k(\nu)}{\sum_{i=0}^n \sum_{j=0}^k \omega_{ij} B_i^n(\mu) B_j^k(\nu)} = \frac{\sum_{i=0}^n \sum_{j=0}^k \omega_{ij} (1 - v_{ij}) B_i^n(\mu) B_j^k(\nu)}{\sum_{i=0}^n \sum_{j=0}^k \omega_{ij} B_i^n(\mu) B_j^k(\nu)}. \tag{54}$$

Since $\mathbf{p}(\mu, \nu)$ is located within the reference tetrahedron, $1 - v_{ij} > 0$ for all i 's. When all ω_{ij} 's are nonnegative,

$$|1 - v(\mu, \nu)| \geq \min_{ij} \{1 - v_{ij}\}.$$

In summary, if c_{ijkl} and ω_{ij} satisfy the above conditions, an upper bound on the approximation accuracy is given by

$$D(\mathbf{p}(\mu, \nu), \text{monoid surface}) \leq \frac{\sigma_1 \max\{\|T_0 T_1\|, \|T_0 T_2\|, \|T_0 T_3\|\}}{\min_{ij} \{1 - v_{ij}\} \min_{i+j+k=n} |c_{ijk0} - i c_{i-1,j,k,1} - j c_{i,j-1,k,1} - k c_{i,j,k-1,1}|}. \tag{55}$$

4.3.3 Error bound for the approximate inversion map

Let the approximate inversion have the form

$$\mu_a = \frac{h(s, t, u, v)}{d(s, t, u, v)}. \quad (56)$$

Compose this with the parametric surface equation (44) so that

$$h(s(\mu, \nu), t(\mu, \nu), u(\mu, \nu)) - vd(s(\mu, \nu), t(\mu, \nu), u(\mu, \nu)) = \epsilon(\mu, \nu), \quad (57)$$

where $|\epsilon(\mu, \nu)| \leq \sigma_\mu$, and σ_μ is the smallest singular value of the composite matrix for the composition of H with the parametric surface. The exact parameter follows directly:

$$\mu_t = \frac{h(s, t, u, v) - \epsilon(\mu, \nu)}{d(s, t, u, v)}, \quad (58)$$

from which an upper bound on the difference between the exact parameter μ_t and the approximate parameter μ_a is:

$$|\mu_t - \mu_a| = \left| \frac{\epsilon(\mu, \nu)}{d(s, t, u, v)} \right| \leq \frac{|\sigma_\mu|}{\min |d(s, t, u, v)|}. \quad (59)$$

By the same token, a bound for parameter ν is found to be

$$|\nu_t - \nu_a| = \left| \frac{\epsilon(\mu, \nu)}{b(s, t, u, v)} \right| \leq \frac{|\sigma_\nu|}{\min |b(s, t, u, v)|}, \quad (60)$$

where σ_ν is the smallest singular value of the composite matrix for the composition of G with the parametric surface. The values of $\min |d(s, t, u, v)|$ and $\min |b(s, t, u, v)|$ can be estimated using the coefficients of polynomials d and b .

5 Examples and discussion

In this section we present examples of the approximate algorithm and discuss its possible applications in compute graphics.

Example 5.1. Consider a degree 3 Bézier curve with control points (2.16, 0.648), (1.92, 0.36), (1.2, 0.2) and (0.0, 1.0). Figure 10 shows an approximate monoid curve (solid line) and the Bézier curve (dash line). Note that there is a self-intersection point when we implicitize this Bézier curve using general algebraic curves as shown in Figure 1.

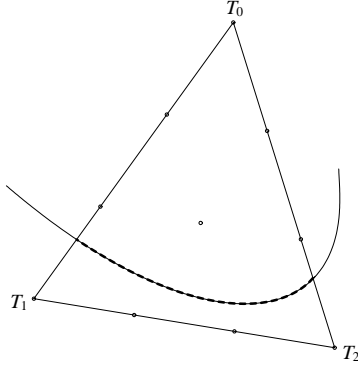


Figure 10: A cubic monoid approximation for a cubic Bézier curve. The approximation error is less than $0.003 \times \text{length}(\text{Bezier curve})$.

Example 5.2. In Figure 11, a degree 4 Bézier curve with control points $(0, 0.4)$, $(1, -1.08)$, $(2, -1.584)$, $(2.92, -1.5792)$ and $(3.712, -1.34512)$ is shown in dash line while its cubic monoid approximation in solid line. Refer to Figure 2 for the exact implicit curve with a “phantom” component.

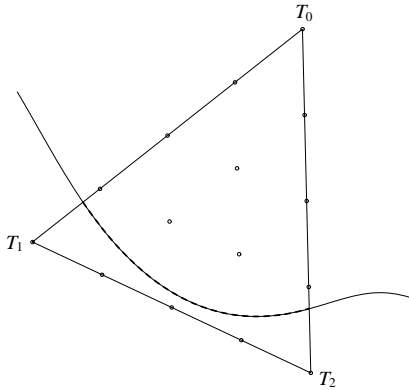


Figure 11: A cubic monoid approximation for a quartic Bézier curve. The approximation error is bounded by $0.0007 \times \text{length}(\text{Bezier curve})$.

These examples show that monoids can closely approximate a parametric curve or surface. Compared with general algebraic curves or surfaces, monoids have fewer degrees of freedom. For example, a degree n monoid curve has $2n + 1$ coefficients, while an algebraic curve of the same degree has $\binom{n+2}{2}$ coefficients. Thus approximation using general algebraic curves or surfaces should converge faster. However, monoids provide an easy way of rejecting the self intersections and other “phantom” branches that are common in general algebraic curves and surfaces. Thus monoids make simple the determination whether a point lies on their inner or outer

side. The relatively complex — and in the case of self-intersecting geometric figures, often ambiguous — parity test, nonexterior rule and nonzero winding number methods used for such point classification can now be replaced by a more straightforward test. Namely, to categorize a given point P with respect to a monoid segment or patch, draw a parametric ray originating at the multiple point of the monoid and going through P , and compare the line parameter values at P with those at the intersection of the line with the curve, as illustrated in Figure 12.

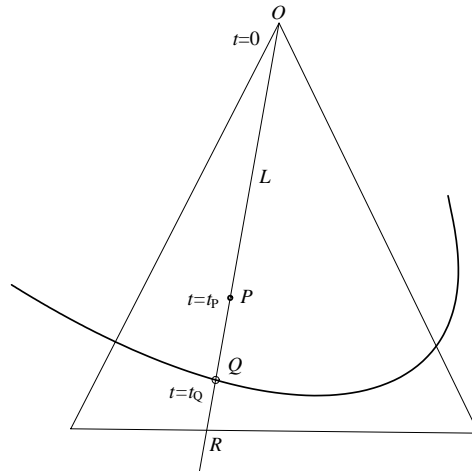


Figure 12: A point on line $L = O + t(R - O)$ lies inside the curve if $t < t_Q$, while a point outside the curve is signified by $t > t_Q$.

One of the possible applications of monoid approximation is ray tracing. This notoriously slow technique for photorealistic image rendering spends up to 95% of time computing ray-object intersections. Objects made of parametric patches are particularly compute-intensive. Monoid approximation provides a new way of computing the intersection(s) between a ray and a parametric surface patch. The basic idea is to first determine a low-degree (usually degree 2, 3 or 4) monoid surface for the patch, then to intersect the ray with the monoid, which amounts to root finding. Once an intersection point between the ray and the monoid is found, the approximate inversion map is used to check whether the intersection is within the parametric patch as well as to compute its parametric coordinates on the patch. Figure 13 explains the process of ray tracing a bicubic patch approximated by a fragment of a monoid surface. Our preliminary tests show that monoid approximation not only faithfully represents objects originally modeled with parametric patches, but also significantly cuts rendering time. The overall intersection time is a factor of two to three times faster than the Bézier clipping method [17].

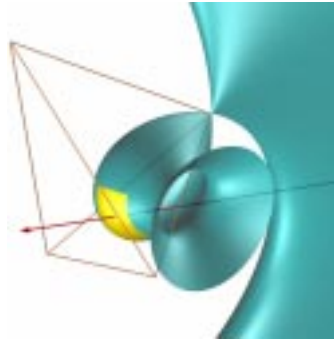


Figure 13: Ray tracing a bicubic patch and the monoid surface. The patch is displayed in yellow. The semi-transparent surface has been clipped to reveal the multiple point. Note the placement of the reference tetrahedron

This paper merely initiates the study of monoid curves and surfaces and their applications in approximate implicitization. There are a number of issues remaining open. One of them is determining the optimal reference triangle or tetrahedron, which is interesting for practical and theoretical reasons. Another one is a theoretical analysis of the convergence rate for the approximation. In addition, in our current implementation, we determine the coefficients of the monoid by computing the eigenvectors, and then checking their values. If they do not satisfy the “same-sign” conditions mentioned in Section 3.1 and Section 4.1, we subdivide the curve or surface, and re-compute the monoids. An alternative approach consisting of finding directly a least-squares solution subject to the “same-sign” condition is also worthy of exploration. Finally, using monoids as a modeling and visualization tool in computer graphics appears to be a promising and interesting proposition that warrants further investigation as well.

Acknowledgments

The first two authors are supported in part by NSF grant number CCR-9712407. The second author is also supported by Doctoral Science Foundation of China.

References

- [1] C. L. Bajaj, J. Chen, and G. Xu. Modeling with cubic A-Patches. *ACM Transactions on Graphics*, 14(2):103–133, April 1995.
- [2] C. L. Bajaj and I. Ihm. Smoothing polyhedra using implicit algebraic splines. In Edwin E. Catmull, editor, *Computer Graphics (SIGGRAPH 92 Conference Proceedings)*, volume 26, pages 79–88, July 1992.
- [3] C. L. Bajaj and G. Xu. Data fitting with cubic A-splines. In *Computer Graphics International*, 1994.
- [4] L. Biard. Parametric surfaces and ray tracing. In *Eurographics Workshop on Photosimulation, Realism and Physics in Computer Graphics*, 1989.
- [5] B. Buchberger. Applications of Gröbner bases in non-linear computational geometry. In J. Rice, editor, *Mathematical Aspects of Scientific Software*. Springer-Verlag, 1988.
- [6] J. H. Chuang and C. M. Hoffmann. On local implicit approximation and its applications. *ACM Transactions on Graphics*, 8(4):298–324, October 1989.
- [7] W. Dahmen. Smooth piecewise quadratic surfaces. In T. Lyche and L. Schumaker, editors, *Mathematical Methods in Computer Aided Geometric Design*, pages 181–193. Academic Press, Boston, 1989.
- [8] W. Dahmen and T-M. Thamm-Schaar. Cubicoids: modeling and visualization. *Computer Aided Geometric Design*, 10:93–108, 1993.
- [9] Y. de Montaudouin, W. Tiller, and H.Vold. Applications of power series in computational geometry. *Computer-Aided Design*, 18(10):93–108, 1986.
- [10] T. D. DeRose, R. Goldman, H. Hagen, and S. Mann. Functional composition algorithms via blossoming. *ACM Transactions on Graphics*, 12(2):113–135, April 1993.
- [11] Tor Dokken. *Aspects of intersection algorithms and approximation*. PhD thesis, University of Oslo, July 1997.
- [12] B. Guo. Surface generation using implicit cubics. In N.M. Patrikalakis, editor, *Scientific Visualization of Physical Phenomena*, pages 485–530. Springer-Verlag, Tokyo, 1991.
- [13] C. M. Hoffmann. *Geometric and Solid Modeling: An Introduction*. Morgan Kaufmann, 1989.

- [14] C. M. Hoffmann. Implicit Curves and Surfaces in CAGD. *IEEE Computer Graphics & Applications*, 13(1):79–88, January 1993.
- [15] J. T. Kajiya. Ray tracing parametric patches. In *Computer Graphics (SIGGRAPH 82 Conference Proceedings)*, volume 16, pages 245–254, July 1982.
- [16] T. L. Kay and J. T. Kajiya. Ray tracing complex scenes. In D. C. Evans and R. J. Athay, editors, *Computer Graphics (SIGGRAPH 86 Conference Proceedings)*, volume 20, pages 269–278, August 1986.
- [17] T. Nishita, T. W. Sederberg, and M. Kakimoto. Ray tracing trimmed rational surface patches. In Forest Baskett, editor, *Computer Graphics (SIGGRAPH 90 Conference Proceedings)*, volume 24, pages 337–345, August 1990.
- [18] T. W. Sederberg. Planar piecewise algebraic curves. *Computer Aided Geometric Design*, 1(3):241–255, 1984.
- [19] T. W. Sederberg. Piecewise algebraic surface patches. *Computer Aided Geometric Design*, 2(1-3):53–60, 1985.
- [20] T. W. Sederberg, D. Anderson, and R. Goldman. Implicit representation of parametric curves and surfaces. *Computer Vision, Graphics, and Image Processing*, 28(1):72–84, 1984.
- [21] T. W. Sederberg and D. C. Anderson. Ray tracing of Steiner patches. In Hank Christiansen, editor, *Computer Graphics (SIGGRAPH 84 Conference Proceedings)*, volume 18, pages 159–164, July 1984.
- [22] T. W. Sederberg and F. Chen. Implicitization using moving curves and surfaces. In Robert Cook, editor, *Computer Graphics (SIGGRAPH 95 Conference Proceedings)*, volume 29, pages 301–308. Addison Wesley, August 1995.
- [23] J. Semple and L. Roth. *Algebraic Geometry*. Clarendon Press, Oxford, 1949.
- [24] D. M. Y. Sommerville. *Analytical Geometry of Three Dimensions*. Cambridge University Press, 1939.
- [25] L. Velho and J. Gomes. Approximate conversion of parametric to implicit surfaces. *Computer Graphics Forum*, 15(5):327–337, 1996. ISSN 0167-7055.
- [26] J. Yen, S. Spach, M. Smith, and R. Pulleyblank. Parallel boxing in B-spline intersection. *IEEE Computer Graphics and Applications*, 11(1):72–79, January 1991.